Full Long-Term Extreme Response Analysis of Marine Structures Using Inverse FORM

Finn-Idar Grøtta Giske[a,b,*], Bernt Johan Leira[a], Ole Øiseth[c]

[a] *Department of Marine Technology, NTNU, 7491 Trondheim, Norway*
[b] *Multiconsult, Nedre Skøyen vei 2, 0213 Oslo, Norway*
[c] *Department of Structural Engineering, NTNU, 7491 Trondheim, Norway*

Abstract

An exact and an approximate formulation for the long-term extreme response of marine structures are discussed and compared. It is well known that the approximate formulation can be evaluated in a simplified way by using the first order reliability method (FORM), known for its computational efficiency. In this paper it is shown how this can be done for the exact formulation as well. Characteristic values of the long-term extreme response are calculated using inverse FORM (IFORM) for both formulations. A new method is proposed for the numerical solution of the IFORM problem, resolving some convergence issues of a well-established iteration algorithm. The proposed method is demonstrated for a single-degree-of-freedom (SDOF) example and the accuracy of the long-term extreme response approximations is investigated, revealing that the IFORM methods provide good estimates in a very efficient manner. The reduced number of required short-term response calculations provided by the IFORM methods is expected to make full long-term extreme response analysis feasible also for more complex systems.

Keywords: marine structures, extreme response, long-term response, stochastic processes, IFORM

*Corresponding author
Email address: finn.i.giske@ntnu.no (Finn-Idar Grøtta Giske)

1. Introduction

For the evaluation of extreme responses in the design of marine structures, a full long-term response analysis is recognized as the most accurate approach [1, 2]. However, the computational effort is in many cases a limiting factor, and simplified approaches such as the environmental contour methods [3, 4, 5] are frequently used in practice. Over the last decade new methods have been proposed in an effort to make the full long-term approach more efficient, either by reducing the required number of short-term response calculations [2, 6, 7] or by computing the short-term quantities more efficiently [8, 9, 10]. In this paper we continue the development of robust and efficient methods for full long-term response analysis.

A comparison of different models for long-term extreme response can be found in [2]. In the present paper we focus on the models based on all short-term extreme peaks. For these models the long-term distribution of the short-term extreme value is formulated as an average of the short-term extreme value distributions weighted by the distribution of the environmental parameters. An exact formulation is obtained when an ergodic averaging is used, but using the population mean yields a very common approximate formulation.

In Section 2 of this paper we compare the exact and the approximate formulation, and show that the latter is non-conservative as it underestimates the long-term extreme responses. Nevertheless, the approximate formulation is commonly used because it readily lends itself to being solved very efficiently in an approximate manner by the first-order reliability method (FORM) known from structural reliability. However, as we show in Section 3, the exact formulation can also be solved using FORM. To the authors' knowledge this has not been done before.

Section 4 deals with the numerical solution of characteristic values for the extreme response using inverse FORM (IFORM). IFORM was introduced in [3] for calculation of extreme response using environmental contours. The IFORM method has also been extended to a more general reliability context [11, 12].

In [2] the IFORM solution for the extreme response of marine structures was found using a simple iteration algorithm proposed in [12]. This iteration algorithm has some convergence issues though, and these are addressed in the present paper. A new method is proposed for dealing with the convergence issues, using a sufficient increase condition along with a backtracking approach for the maximization problem being solved. It should be mentioned that an exact arc search algorithm [13] can also be used to obtain convergence, but this approach is expected to require a larger number of short-term response calculations. Furthermore, the proposed method is simpler in its form and will be easier to implement.

In Sections 5 and 6 a single-degree-of-freedom (SDOF) example is given, demonstrating the use of the proposed method. Some numerical results are also presented in order to compare the method with the standard iteration algorithm, and to assess the accuracy of the approximate formulation and the IFORM approximations.

2. Long-term extreme response modelling

For the assessment of long-term extreme responses of marine structures, it is common to model the environmental conditions as a sequence of short-term states during which the environmental processes are assumed stationary [1]. Each short-term state is defined by a collection of environmental parameters $\boldsymbol{S} = [S_1, S_2, \ldots, S_n]$, with a joint probability density function (PDF) $f_{\boldsymbol{S}}(\boldsymbol{s})$ which we assume is given. We note that in order to be able to estimate $f_{\boldsymbol{S}}(\boldsymbol{s})$ in practice, an ergodicity assumption is required for the environmental parameters [14]. The long-term situation is composed of a large number N of short-term conditions, each of duration $\tilde{T}$, giving a long-term time duration of $T = N\tilde{T}$.

We denote by $\tilde{R}$ the largest peak of the response process during an arbitrary short-term condition, and by $\tilde{R}_{LT}$ the largest peak during the entire long-term period. Assuming that the short-term extreme values are independent, the long-term extreme value distribution $F_{\tilde{R}_{LT}}(r)$ is obtained as

$$F_{\tilde{R}_{LT}}(r) = F_{\tilde{R}}(r)^{N}, \tag{1}$$

where $F_{\tilde{R}}(r)$ is the cumulative distribution function (CDF) of the short-term extreme value $\tilde{R}$.

2.1. Formulations based on the short-term extreme peaks

Let the CDF of the largest peak during a short-term condition with environmental parameters $\boldsymbol{s}$ be given by $F_{\tilde{R}|\boldsymbol{S}}(r|\boldsymbol{s})$. The exact long-term CDF $F_{\tilde{R}}(r)$ of the short-term extreme value is obtained when an ergodic averaging is used [14, 15], see also Section 12.4.2 of [1]. Thus we have the formulation

$$F_{\tilde{R}}(r) = \exp\left\{\int_{\boldsymbol{s}} \left(\ln F_{\tilde{R}|\boldsymbol{S}}(r|\boldsymbol{s})\right) f_{\boldsymbol{S}}(\boldsymbol{s})\, d\boldsymbol{s}\right\}. \tag{2}$$

The claim of exactness for the formulation (2) is perhaps somewhat unfortunate, since e.g. the assumption of stationary environmental processes is clearly not exact. The term "exact" is simply used here in the sense that the formulation (2) is the mathematically correct approach within the assumptions.

Usually, we are only interested in $F_{\tilde{R}}(r)$ for large values of r, which means that $F_{\tilde{R}|\boldsymbol{S}}(r|\boldsymbol{s}) \approx 1$. Using the linear approximations of the logarithm and the exponential function yields

$$F_{\tilde{R}}(r) \approx \exp\left\{-\int_{\boldsymbol{s}} \left(1 - F_{\tilde{R}|\boldsymbol{S}}(r|\boldsymbol{s})\right) f_{\boldsymbol{S}}(\boldsymbol{s})\, d\boldsymbol{s}\right\} \approx 1 - \int_{\boldsymbol{s}} \left(1 - F_{\tilde{R}|\boldsymbol{S}}(r|\boldsymbol{s})\right) f_{\boldsymbol{S}}(\boldsymbol{s})\, d\boldsymbol{s}.$$

From the properties of a PDF we know that the integral of $f_{\boldsymbol{S}}(\boldsymbol{s})$ over all values of $\boldsymbol{s}$ equals unity, and we obtain the approximation $F_{\tilde{R}}(r) \approx \bar{F}_{\tilde{R}}(r)$, where $\bar{F}_{\tilde{R}}(r)$ is the population mean

$$\bar{F}_{\tilde{R}}(r) = \int_{\boldsymbol{s}} F_{\tilde{R}|\boldsymbol{S}}(r|\boldsymbol{s})\, f_{\boldsymbol{S}}(\boldsymbol{s})\, d\boldsymbol{s}. \tag{3}$$

The formulation (3) is a common approximation for the long-term CDF of the short-term extreme value, partly because it readily lends itself to being solved very efficiently by the FORM method. Furthermore, it is easy to mistakenly consider (3) as exact, because the formulation intuitively appears to be correct.

2.2. Connection with the average upcrossing rate formulation

If we assume that upcrossings of high levels are statistically independent, the short-term extreme peak distribution is given by

$$F_{\tilde{R}|\boldsymbol{S}}\left(r|\boldsymbol{s}\right) = \exp\left\{-\nu\left(r|\boldsymbol{s}\right)\tilde{T}\right\}, \tag{4}$$

where $\nu(r|\boldsymbol{s})$ denotes the short-term mean frequency of r-upcrossings. For details we refer to Section 10.5 of [1]. Note that the expression (4) is only valid for high levels, i.e. for relatively large values of r. Inserting the expression (4) into (2) yields

$$F_{\tilde{R}}\left(r\right) = \exp\left\{-\tilde{T}\int_{\boldsymbol{s}}\nu\left(r|\boldsymbol{s}\right)f_{\boldsymbol{S}}\left(\boldsymbol{s}\right)d\boldsymbol{s}\right\}, \tag{5}$$

and the relation (1) for the long-term extreme value distribution $F_{\tilde{R}_{LT}}(r)$ gives that

$$F_{\tilde{R}_{LT}}\left(r\right) = \exp\left\{-T\int_{\boldsymbol{s}}\nu\left(r|\boldsymbol{s}\right)f_{\boldsymbol{S}}\left(\boldsymbol{s}\right)d\boldsymbol{s}\right\}, \tag{6}$$

where $T = N\tilde{T}$ is the long-term period. The expression (6) is also a common model for the long-term extreme response [14]. The fact that (2) and (6) are equivalent formulations is in agreement with what is found in [2].

2.3. Non-conservativity of the approximate formulation

As a simple consequence of Jensen's inequality, it can be show that $\bar{F}_{\tilde{R}}(r) > F_{\tilde{R}}(r)$. Indeed, since the natural logarithm is a strictly concave function, Jensen's inequality yields

$$\ln\left(E\left[F_{\tilde{R}|\boldsymbol{S}}\left(r|\boldsymbol{S}\right)\right]\right) > E\left[\ln\left(F_{\tilde{R}|\boldsymbol{S}}\left(r|\boldsymbol{S}\right)\right)\right],$$

where $E[\cdot]$ denotes the expectation operator. From (2) and (3) we realize that $\ln\left(F_{\tilde{R}}\left(r\right)\right) = E\left[\ln\left(F_{\tilde{R}|\boldsymbol{S}}\left(r|\boldsymbol{S}\right)\right)\right]$ and $\bar{F}_{\tilde{R}}\left(r\right) = E\left[F_{\tilde{R}|\boldsymbol{S}}\left(r|\boldsymbol{S}\right)\right]$, which means that $\ln\left(\bar{F}_{\tilde{R}}\left(r\right)\right) > \ln\left(F_{\tilde{R}}\left(r\right)\right)$ and hence $\bar{F}_{\tilde{R}}(r) > F_{\tilde{R}}(r)$.

From the result $\bar{F}_{\tilde{R}}(r) > F_{\tilde{R}}(r)$, it follows that exceedance probabilities will be smaller for the approximate formulation (3) compared to the exact formulation (2). This means that the formulation (3) will underestimate the long-term extreme values, making it a non-conservative approximation. Although the underestimation might not be significant, it is important to be aware of such an issue.

3. FORM formulations for long-term extremes

In this section we will show how the integrals of both formulations (2) and (3) can be solved in an approximate manner using the first order reliability method (FORM) found in connection with structural reliability analysis. In order to employ the FORM method, the formulations have to be rewritten in terms of a reliability problem. A reliability problem in the general sense is an integral written in the form

$$p_f = \int\limits_{G(\boldsymbol{v})\leq 0} f_{\boldsymbol{V}}\left(\boldsymbol{v}\right) d\boldsymbol{v},$$

where $\boldsymbol{V}$ is a random vector with joint PDF $f_{\boldsymbol{V}}(\boldsymbol{v})$ [16]. Using reliability analysis terminology, the function $G(\boldsymbol{v})$ is referred to as the limit state function and the value of the integral p_f is called the failure probability.

3.1. Expressing the approximate formulation in terms of a reliability problem

That the integral (3) can be rewritten as a reliability problem, is well known. This is done by first rewriting

$$\bar{F}_{\tilde{R}}\left(r\right) = \int_{\boldsymbol{s}} F_{\tilde{R}|\boldsymbol{S}}\left(r|\boldsymbol{s}\right) f_{\boldsymbol{S}}\left(\boldsymbol{s}\right) d\boldsymbol{s} = \int_{\boldsymbol{s}}\int_{\tilde{r}\leq r} f_{\tilde{R}|\boldsymbol{S}}\left(\tilde{r}|\boldsymbol{s}\right) d\tilde{r} f_{\boldsymbol{S}}\left(\boldsymbol{s}\right) d\boldsymbol{s}.$$

We then define the random vector $\boldsymbol{V} = [\boldsymbol{S}, \tilde{R}]$, whose joint PDF will be $f_{\boldsymbol{V}}\left(\boldsymbol{v}\right) = f_{\tilde{R}|\boldsymbol{S}}\left(\tilde{r}|\boldsymbol{s}\right) f_{\boldsymbol{S}}\left(\boldsymbol{s}\right)$. Thus we have

$$\bar{F}_{\tilde{R}}\left(r\right) = \int\limits_{\tilde{r}\leq r} f_{\boldsymbol{V}}\left(\boldsymbol{v}\right) d\boldsymbol{v} = 1 - \int\limits_{r-\tilde{r}\leq 0} f_{\boldsymbol{V}}\left(\boldsymbol{v}\right) d\boldsymbol{v},$$

and defining the limit state function $G_r\left(\boldsymbol{v}\right) = r - \tilde{r} = r - v_{n+1}$ we end up with

$$\bar{F}_{\tilde{R}}\left(r\right) = 1 - \int\limits_{G_r(\boldsymbol{v})\leq 0} f_{\boldsymbol{V}}\left(\boldsymbol{v}\right) d\boldsymbol{v} = 1 - p_f(r), \tag{7}$$

where $p_f(r)$ is the failure probability.

3.2. *Expressing the exact formulation in terms of a reliability problem*

The integral in (2) can not directly be rewritten as a reliability problem using the same approach as in Section 3.1, due to the fact that the factor $\left(\ln F_{\tilde{R}|\boldsymbol{S}}\left(r|\boldsymbol{s}\right)\right)$ is not a CDF. However, the expression (2) can be rewritten as

$$F_{\tilde{R}}\left(r\right) = \exp\left\{\int_{\boldsymbol{s}} \left(1 + \ln\left(F_{\tilde{R}|\boldsymbol{S}}\left(r|\boldsymbol{s}\right)\right)\right) f_{\boldsymbol{S}}\left(\boldsymbol{s}\right) d\boldsymbol{s} - 1\right\}. \tag{8}$$

Now, for reasonably high levels r we have that the value of $F_{\tilde{R}|\boldsymbol{S}}\left(r|\boldsymbol{s}\right)$ will be close to one, but always less than one, and hence its logarithm is negative and close to zero. This means that $1 + \ln\left(F_{\tilde{R}|\boldsymbol{S}}\left(r|\boldsymbol{s}\right)\right)$ can be viewed as a CDF for values of r such that $F_{\tilde{R}|\boldsymbol{S}}\left(r|\boldsymbol{s}\right) \geq \exp\{-1\}$, and for any given short-term condition $\boldsymbol{S}$ we can introduce the random variable Y whose CDF is given by

$$F_{Y|\boldsymbol{S}}\left(y|\boldsymbol{s}\right) = \max\left\{1 + \ln\left(F_{\tilde{R}|\boldsymbol{S}}\left(y|\boldsymbol{s}\right)\right), 0\right\}. \tag{9}$$

An example of the CDF $F_{Y|\boldsymbol{S}}(y|\boldsymbol{s})$ is given in Figure 1, demonstrating how $1 + \ln\left(F_{\tilde{R}|\boldsymbol{S}}(r|\boldsymbol{s})\right)$ can be viewed as a CDF for sufficiently large r. When considering long-term extreme values r, the main contribution to the integral in (8) will be for values of $\boldsymbol{s}$ where $F_{Y|\boldsymbol{S}}\left(r|\boldsymbol{s}\right) = 1 + \ln\left(F_{\tilde{R}|\boldsymbol{S}}\left(r|\boldsymbol{s}\right)\right)$, and we obtain

$$F_{\tilde{R}}\left(r\right) \approx \exp\left\{\int_{\boldsymbol{s}} F_{Y|\boldsymbol{S}}\left(r|\boldsymbol{s}\right) f_{\boldsymbol{S}}\left(\boldsymbol{s}\right) d\boldsymbol{s} - 1\right\}. \tag{10}$$

For long-term extreme values r, (10) is expected to be a much better approximation to the exact long-term CDF than the formulation (3). This is because $F_{Y|\boldsymbol{S}}(r|\boldsymbol{s})$ exactly represents $1 + \ln\left(F_{\tilde{R}|\boldsymbol{S}}\left(r|\boldsymbol{s}\right)\right)$ for the relevant values of r, whereas $F_{\tilde{R}|\boldsymbol{S}}(r|\boldsymbol{s})$ is an approximation also for larger values of r as seen in Figure 1. Now the integral (10) can be rewritten using the same approach as in Section 3.1, giving

$$F_{\tilde{R}}\left(r\right) \approx \exp\left\{-\int_{G_r(\boldsymbol{v})\leq 0} f_{\boldsymbol{V}}\left(\boldsymbol{v}\right) d\boldsymbol{v}\right\} = \exp\left\{-p_f\left(r\right)\right\}, \tag{11}$$

where the failure probability $p_f(r)$ now is obtained using $V_{n+1} = Y$ instead of $V_{n+1} = \tilde{R}$ as in Section 3.1.

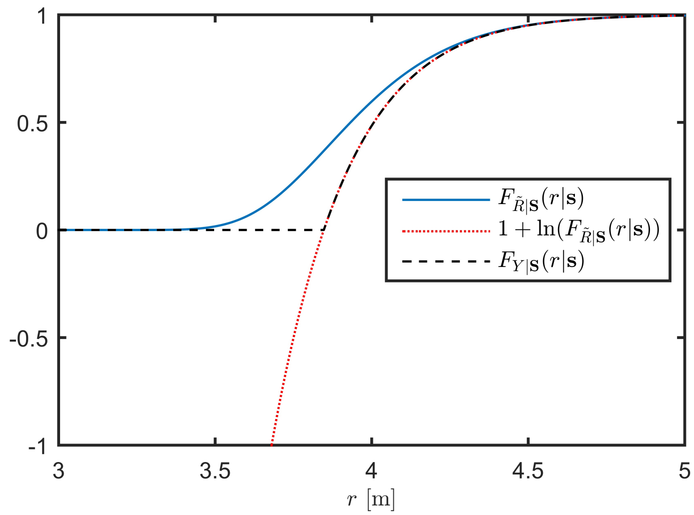

Figure 1: An example of the CDF $F_{Y|\boldsymbol{S}}(y|\boldsymbol{s})$ as given by (9), along with the short-term extreme value distribution $F_{\tilde{R}|\boldsymbol{S}}(r|\boldsymbol{s})$ and $1+\ln\left(F_{\tilde{R}|\boldsymbol{S}}(r|\boldsymbol{s})\right)$.

3.3. Finding the failure probability using FORM

The problem of finding the failure probability $p_f(r)$ in (7) and (11) can be solved for a given exceedance level r using the FORM method. The random vector $\boldsymbol{V}$ is transformed into a vector $\boldsymbol{U}$ of independent standard normal variables by the Rosenblatt transformation $\boldsymbol{U} = T(\boldsymbol{V})$ [16], defined by the equations

$$\Phi\left(U_1\right) = F_{V_1}\left(V_1\right), \tag{12a}$$

$$\Phi\left(U_i\right) = F_{V_i|V_1,\ldots,V_{i-1}}\left(V_i|V_1,\ldots,V_{i-1}\right), i = 2,\ldots,n, \tag{12b}$$

$$\Phi\left(U_{n+1}\right) = F_{V_{n+1}|V_1,\ldots,V_n}\left(V_{n+1}|V_1,\ldots,V_n\right), \tag{12c}$$

where Φ denotes the standard normal CDF. Given a point $\boldsymbol{u}$ in the standard normal space, the inverse transformation evaluated at $\boldsymbol{u}$, i.e. $\boldsymbol{v} = T^{-1}(\boldsymbol{u})$, can be found by solving the equations (12) successively, obtaining

$$v_1\left(\boldsymbol{u}\right) = F_{V_1}^{-1}\left(\Phi\left(u_1\right)\right), \tag{13a}$$

$$v_i\left(\boldsymbol{u}\right) = F_{V_i|V_1,\ldots,V_{i-1}}^{-1}\left(\Phi\left(u_i\right)|v_1\left(\boldsymbol{u}\right),\ldots,v_{i-1}\left(\boldsymbol{u}\right)\right), \tag{13b}$$

$$v_{n+1}\left(\boldsymbol{u}\right) = F_{V_{n+1}|V_1,\ldots,V_n}^{-1}\left(\Phi\left(u_{n+1}\right)|v_1\left(\boldsymbol{u}\right),\ldots,v_n\left(\boldsymbol{u}\right)\right). \tag{13c}$$

The failure probability integral is then rewritten in terms of the transformed variables as

$$p_f(r) = \int_{G_r(\boldsymbol{v})\leq 0} f_{\boldsymbol{V}}(\boldsymbol{v})\, d\boldsymbol{v} = \int_{g_r(\boldsymbol{u})\leq 0} f_{\boldsymbol{U}}(\boldsymbol{u})\, d\boldsymbol{u}, \tag{14}$$

where the transformed limit state function is $g_r(\boldsymbol{u}) = G_r\left(T^{-1}(\boldsymbol{u})\right) = r - v_{n+1}(\boldsymbol{u})$. Now if $g_r(\boldsymbol{u})$ is a linear function, we have that

$$p_f(r) = \int_{g_r(\boldsymbol{u})\leq 0} f_{\boldsymbol{U}}(\boldsymbol{u})\, d\boldsymbol{u} = \Phi(-\beta), \tag{15}$$

where β is the distance from the origin to the $(n+1)$-dimensional hyperplane defined by $g_r(\boldsymbol{u}) = 0$.

The idea behind the FORM procedure is that, assuming that the failure probability is small, the formula (15) will still hold in an approximate sense even if $g_r(\boldsymbol{u})$ is not linear. The value β must then be found by solving the optimization problem

$$\beta = \min|\boldsymbol{u}|;\ \text{subject to}\ g_r(\boldsymbol{u}) = 0. \tag{16}$$

The minimizer $\boldsymbol{u}^*$ satisfying $|\boldsymbol{u}^*| = \beta$ is also found in the procedure, and the transformed point $\boldsymbol{v}^* = T^{-1}(\boldsymbol{u}^*)$ is referred to as the design point.

If $\bar{\beta}_r$ denotes the solution of the minimization problem (16) when $V_{n+1} = \tilde{R}$, we have from (7) and (15) that

$$\bar{F}_{\tilde{R}}(r) \approx 1 - \Phi(-\bar{\beta}_r). \tag{17}$$

Similarly, if β_r denotes the solution of the minimization problem (16) when $V_{n+1} = Y$, we have from (11) and (15) that

$$F_{\tilde{R}}(r) \approx \exp\left\{-\Phi(-\beta_r)\right\}. \tag{18}$$

4. Solution of the extreme response by use of inverse FORM (IFORM)

4.1. Finding the design point using inverse FORM

As seen in Section 3, the CDFs $\bar{F}_{\tilde{R}}(r)$ and $F_{\tilde{R}}(r)$ can be evaluated at a given level r using FORM. However, when designing a structure one is commonly faced with the inverse problem of finding the characteristic response level r corresponding to a given exceedance probability. For instance, the M-year extreme response r_M is defined as the response level with a return period of M years. This is found by requiring that the exceedance probability per year is $1/M$, i.e. $F_{\tilde{R}_{LT}}(r_M) = 1 - 1/M$ for a long-term period of one year. Using the relation (1), the equation for r_M can be expressed in terms of the short-term extreme value distribution as

$$F_{\tilde{R}}(r_M) = \left(1 - \frac{1}{M}\right)^{1/N} \approx 1 - \frac{1}{MN},$$

since the number of short-term periods N is large. If the short-term period $\tilde{T}$ is three hours and the long-term period T is one year, we have $N = 365 \cdot 8 = 2920$. As an example, the 100-year extreme response r_{100} then corresponds to the exceedance probability $1 - F_{\tilde{R}}(r_{100}) = 1/292000$.

When the exceedance probability is specified, the corresponding reliability index β in the FORM procedure is given by solving for $\bar{\beta}_r$ in (17) or β_r in (18) for the approximate and exact formulations respectively. Instead we have to find the value r_M such that the limit surface defined by $g_{r_M}(\boldsymbol{u}) = r_M - v_{n+1}(\boldsymbol{u}) = 0$, where $v_{n+1}(\boldsymbol{u})$ is given in (13), has a minimal distance β to the origin. According to [3, 13] this inverse FORM (IFORM) problem can be formulated as

$$r_M = \max v_{n+1}(\boldsymbol{u}); \text{ subject to } |\boldsymbol{u}| = \beta. \tag{19}$$

Using the method of Lagrange multipliers, we recognize that for both the problems (16) and (19) an optimal point $\boldsymbol{u}^*$ must satisfy

$$\frac{\boldsymbol{u}^*}{|\boldsymbol{u}^*|} = \frac{\nabla v_{n+1}(\boldsymbol{u}^*)}{|\nabla v_{n+1}(\boldsymbol{u}^*)|}, \tag{20}$$

in addition to the constraint of the specific problem. Thus, if $\boldsymbol{u}^*$ is a solution to the problem (19), it satisfies (20) and $|\boldsymbol{u}^*| = \beta$. Furthermore, r_M is given by $r_M = v_{n+1}(\boldsymbol{u}^*)$, so $g_{r_M}(\boldsymbol{u}^*) = r_M - v_{n+1}(\boldsymbol{u}^*) = 0$ and the constraint in (16) is also satisfied. Assuming that (16) has a unique solution, this shows that $\boldsymbol{u}^*$ is the minimizer for the problem (16) and β is indeed the minimal distance from the origin to the limit surface $g_{r_M}(\boldsymbol{u}) = r_M - v_{n+1}(\boldsymbol{u}) = 0$. In other words, a solution to the problem (19) is a solution to the IFORM problem.

4.2. Existing solution algorithms for the IFORM problem

A solution algorithm for the IFORM problem (19), which aims at solving (20) with $|\boldsymbol{u}^*| = \beta$ in an iterative manner, is proposed in [12] and applied in [2]. This iteration is given by

$$\boldsymbol{u}^{k+1} = \beta \frac{\nabla v_{n+1}\left(\boldsymbol{u}^k\right)}{\left|\nabla v_{n+1}\left(\boldsymbol{u}^k\right)\right|}. \tag{21}$$

It can be shown that this is the same as using the steepest ascent method (equivalent to the steepest descent method for minimization) searching for the optimal point, i.e. the maximizer of $v_{n+1}(\boldsymbol{u})$, on the hypersphere with radius β. The gradient $\nabla v_{n+1}(\boldsymbol{u}^k)$ is projected onto the tangent plane of the sphere at the point $\boldsymbol{u}^k$, giving the direction on the sphere along which the function $v_{n+1}(\boldsymbol{u})$ increases most rapidly. The optimal point is then searched for along an arc on the sphere that follows this search direction. The updated point $\boldsymbol{u}^{k+1}$ is found as the point that maximizes $v_{n+1}(\boldsymbol{u})$ along this arc, when approximating the gradient $\nabla v_{n+1}(\boldsymbol{u})$ as constant equal to $\nabla v_{n+1}(\boldsymbol{u}^k)$. This is illustrated very nicely in [13].

The iteration (21) is very simple and easy to use. However, it may fail to converge to the optimal point. Due to the approximation of constant gradient $\nabla v_{n+1}(\boldsymbol{u})$ along the search direction, the updated point $\boldsymbol{u}^{k+1}$ is not guaranteed to give a sufficient increase of $v_{n+1}(\boldsymbol{u})$ and it may even give a decrease. This problem was addressed in [13] by performing an exact arc search whenever an iteration point given by (21) would give a decrease. The exact arc search must be performed by solving a one-dimensional optimization problem, which might require a relatively large number of function evaluations without a significant gain in the convergence rate. In the context of the present paper we strive to limit the number of function evaluations, since each function evaluation corresponds to a possibly very time-consuming short-term response analysis. Hence, a simpler method for achieving convergence is preferred.

It should be mentioned that, as an alternative, the IFORM problem (19) can be recast in terms of angles, resulting in in "box-like" constraints [3]. A variety of optimization algorithms can be used to solve such a problem efficiently. In this paper, however, we pursue a further development of the simple iteration (21) which is easy to implement.

4.3. A new solution algorithm for the IFORM problem

A simple method that resolves the convergence issues, while keeping the number of function evaluation to a minimum, is obtained by using a sufficient increase condition along with a backtracking approach, similar to what is explained in Chapter 3.1 of [17]. We require that the increase of $v_{n+1}(\boldsymbol{u})$ when going from $\boldsymbol{u}^k$ to the updated point $\boldsymbol{u}^{k+1}$ is proportional to the step length and the directional derivative at $\boldsymbol{u}^k$ along the search direction, this is known as the Armijo condition [17, 18]. In our case the sufficient increase condition requires $\boldsymbol{u}^{k+1}$ to satisfy

$$v_{n+1}\left(\boldsymbol{u}^{k+1}\right) - v_{n+1}\left(\boldsymbol{u}^{k}\right) \geq cd\alpha. \tag{22}$$

Here $c \in (0,1)$ is a proportionality constant chosen as $c = 10^{-4}$ in this paper, d is the directional derivative at $\boldsymbol{u}^k$ and α is the step length measured as the distance between $\boldsymbol{u}^k$ and $\boldsymbol{u}^{k+1}$ along the sphere. These are given respectively by

$$d = \frac{1}{\beta}\sqrt{\beta^2\left|\nabla v_{n+1}\left(\boldsymbol{u}^k\right)\right|^2 - \left(\boldsymbol{u}^k \cdot \nabla v_{n+1}\left(\boldsymbol{u}^k\right)\right)^2}, \tag{23}$$

and

$$\alpha = \beta \cos^{-1}\frac{\boldsymbol{u}^k \cdot \nabla v_{n+1}\left(\boldsymbol{u}^k\right)}{\beta\left|\nabla v_{n+1}\left(\boldsymbol{u}^k\right)\right|}, \tag{24}$$

where the dot denotes the dot product of two vectors.

A solution algorithm for the IFORM problem (19) where the iteration points satisfy the sufficient increase condition (22) is given by Algorithm 1. At each iteration the algorithm starts by trying $\boldsymbol{u}^{k+1}$ as given by (21), and if sufficient increase is not achieved, the backtracking approach is employed by halving the step length successively until the sufficient increase condition is satisfied. In Algorithm 1 choices have to be made for the initial point $\boldsymbol{u}^1$ and for the tolerance *Tol* of the convergence criterion $\frac{|\boldsymbol{u}^{k+1}-\boldsymbol{u}^k|}{|\boldsymbol{u}^{k+1}|} < Tol$. In this paper $\boldsymbol{u}^1 = [\boldsymbol{0}, \beta]$ and $Tol = 10^{-3}$ have been used. These choices serve to demonstrate the efficiency of the method, but other choices may be more appropriate and give faster convergence.

Algorithm 1 Solution algorithm for the IFORM problem (19) where the iteration points satisfy the sufficient increase condition (22).

Choose $Tol > 0$ and $\boldsymbol{u}^1$ with $|\boldsymbol{u}^1| = \beta$;

Set $Convergence \leftarrow$ FALSE;

Set $k \leftarrow 1$;

while $Convergence$ = FALSE **do**

  Choose $c \in (0, 1)$;

  Evaluate $v_{n+1}(\boldsymbol{u}^k)$ and $\nabla v_{n+1}(\boldsymbol{u}^k)$;

  Calculate directional derivative d using (23);

  Calculate initial step length α using (24);

  $\boldsymbol{u}^{k+1} \leftarrow \beta \frac{\nabla v_{n+1}(\boldsymbol{u}^k)}{|\nabla v_{n+1}(\boldsymbol{u}^k)|}$;

  Evaluate $v_{n+1}(\boldsymbol{u}^{k+1})$;

  while $v_{n+1}\left(\boldsymbol{u}^{k+1}\right) - v_{n+1}\left(\boldsymbol{u}^k\right) < cd\alpha$ **do**

    $\alpha \leftarrow \alpha/2$;

    $\boldsymbol{u}^{k+1} \leftarrow \beta \frac{\boldsymbol{u}^{k+1}+\boldsymbol{u}^k}{|\boldsymbol{u}^{k+1}+\boldsymbol{u}^k|}$;

    Evaluate $v_{n+1}(\boldsymbol{u}^{k+1})$;

  end while

  if $\frac{|\boldsymbol{u}^{k+1}-\boldsymbol{u}^k|}{|\boldsymbol{u}^{k+1}|} < Tol$ **then**

    $\boldsymbol{u}^* \leftarrow \boldsymbol{u}^{k+1}$;

    $Convergence \leftarrow$ TRUE;

  end if

  Set $k \leftarrow k + 1$;

end while

5. An SDOF example

5.1. The response model

As an example we consider the stochastic response $R(t)$ of a linear, time-invariant single-degree-of-freedom (SDOF) system due to a wave elevation process $\eta(t)$, which is assumed to be stationary and Gaussian with zero mean for given environmental parameters $\boldsymbol{s}$. This means that, given $\boldsymbol{s}$, $R(t)$ will also be stationary and Gaussian with zero mean. The SDOF system is described in the frequency domain by the transfer function

$$H_{\eta R}(\omega) = \left(1 - \left(\frac{\omega}{\omega_n}\right)^2 + i2\zeta\frac{\omega}{\omega_n}\right)^{-1},$$

where $\zeta = 0.05$ is the damping ratio and ω_n is the natural frequency. We use the environmental parameters $\boldsymbol{S} = [H_s, T_z]$, where H_s is the significant wave height and T_z is the zero-crossing period, and specify the wave elevation process by the generalized Pierson-Moskowitz spectrum [19] given by

$$S_{\eta|\boldsymbol{S}}(\omega|\boldsymbol{s}) = S_{\eta|H_s,T_z}(\omega|h_s,t_z) = \frac{{h_s}^2 t_z}{8\pi^2}\left(\frac{\omega t_z}{2\pi}\right)^{-5} \exp\left\{-\frac{1}{\pi}\left(\frac{\omega t_z}{2\pi}\right)^{-4}\right\}.$$

Now the response spectrum $S_{R|\boldsymbol{S}}(\omega|\boldsymbol{s})$ is obtained by the well known relationship [1]

$$S_{R|\boldsymbol{S}}(\omega|\boldsymbol{s}) = |H_{\eta R}(\omega)|^2 S_{\eta|\boldsymbol{S}}(\omega|\boldsymbol{s}).$$

Figure 2 shows the wave spectrum $S_\eta(\omega)$ plotted in the nondimensional scale $\omega T_z/2\pi$. Figure 3 shows the absolute value $|H_{\eta R}(\omega)|$ of the transfer function for different values of $\omega_n T_z/2\pi$ using the same scale as for the wave spectrum.

5.2. The environmental model

The CDF of the significant wave height H_s is given by a 2-parameter Weibull distribution

$$F_{H_s}(h) = 1 - \exp\left\{-\left(\frac{h}{\alpha}\right)^\beta\right\}, \tag{25}$$

and the zero-crossing period T_z has a conditioned lognormal distribution

$$F_{T_z|H_s}(t|h) = \Phi\left(\frac{\ln t - \mu(h)}{\sigma(h)}\right), \tag{26}$$

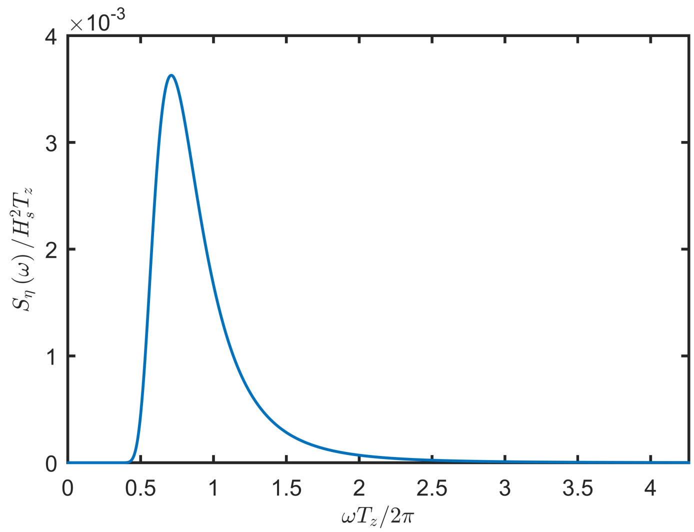

Figure 2: The generalized Pierson-Moskowitz spectrum.

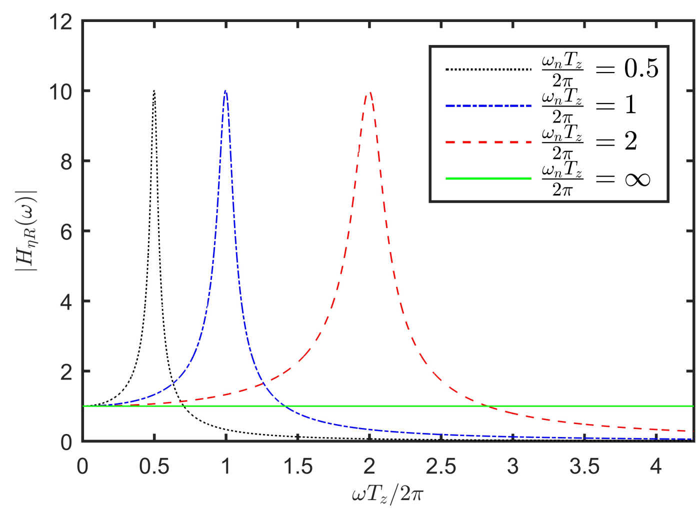

Figure 3: The absolute value $|H_{\eta R}(\omega)|$ of the transfer function.

where $\mu(h) = a_0 + a_1 h^{a_2}$ and $\sigma(h) = b_0 + b_1 e^{b_2 h}$. This is a model for the environmental parameters that is recommended in [20], and in this paper we use the parameter values $\alpha = 1.76$, $\beta = 1.59$, $a_0 = 0.70$, $a_1 = 0.282$, $a_2 = 0.167$, $b_0 = 0.07$, $b_1 = 0.3449$ and $b_2 = -0.2073$. The PDFs $f_{H_s}(h)$ and $f_{T_z|H_s}(t|h)$ can be obtained by differentiating (25) and (26) with respect to h and t respectively, giving the joint PDF of the environmental parameters as

$$f_{\boldsymbol{S}}(\boldsymbol{s}) = f_{H_s,T_z}(h,t) = f_{H_s}(h)\, f_{T_z|H_s}(t|h)\,.$$

This way of establishing the joint environmental model is referred to as the conditional modelling approach [20, 21]. The joint PDF $f_{\boldsymbol{S}}(\boldsymbol{s}) = f_{H_s,T_z}(h,t)$ is presented in Figure 4.

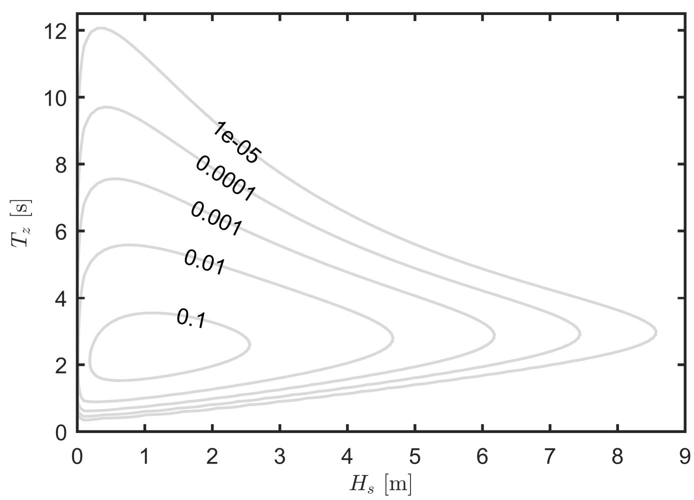

Figure 4: The joint PDF of the environmental parameters presented by its isoprobability contours.

5.3. The short-term extreme value distribution

Since $R(t)|\boldsymbol{S}$ is stationary and Gaussian with zero mean, the mean frequency of r-upcrossings is given by

$$\nu(r|\boldsymbol{s}) = \frac{1}{2\pi}\sqrt{\frac{m_2(\boldsymbol{s})}{m_0(\boldsymbol{s})}}\exp\left\{-\frac{r^2}{2m_0(\boldsymbol{s})}\right\},$$

where the ith moment $m_i(\boldsymbol{s})$ of the response spectrum $S_{R|\boldsymbol{S}}(\omega|\boldsymbol{s})$ is defined as

$$m_i\left(\boldsymbol{s}\right) = \int_0^\infty \omega^i S_{R|\boldsymbol{S}}\left(\omega|\boldsymbol{s}\right) d\omega. \tag{27}$$

Now if $\tilde{R}|\boldsymbol{S}$ denotes the largest value of the response process $R(t)$ during a short term period of $\tilde{T} = 3\text{h}$ with given environmental parameters, and we assume independent upcrossings of high levels, then the short-term extreme peak CDF is given by (4). Thus we have the expression

$$F_{\tilde{R}|\boldsymbol{S}}\left(r|\boldsymbol{s}\right) = \exp\left\{-\nu\left(r|\boldsymbol{s}\right)\tilde{T}\right\} = \exp\left\{-\frac{\tilde{T}}{2\pi}\sqrt{\frac{m_2\left(\boldsymbol{s}\right)}{m_0\left(\boldsymbol{s}\right)}}\exp\left\{-\frac{r^2}{2m_0\left(\boldsymbol{s}\right)}\right\}\right\}, \tag{28}$$

which holds for reasonably large values of r.

5.4. The FORM formulations

In this example we have that $\boldsymbol{V} = [\boldsymbol{S}, V_3] = [H_s, T_z, V_3]$, where $V_3 = \tilde{R}$ for the FORM formulation (7) in Section 3.1, whereas $V_3 = Y$ for the FORM formulation (11) in Section 3.2. Now given a point $\boldsymbol{u} = [u_1, u_2, u_3]$ in the standard normal space, the corresponding point $\boldsymbol{v} = [h(\boldsymbol{u}), t(\boldsymbol{u}), v_3(\boldsymbol{u})] = T^{-1}(\boldsymbol{u})$ is evaluated using (13), which in this case takes the form

$$\begin{aligned}
h(\boldsymbol{u}) &= F_{H_s}^{-1}\left(\Phi\left(u_1\right)\right) = \alpha[-\ln\left(1-\Phi\left(u_1\right)\right)]^{1/\beta}, \\
t(\boldsymbol{u}) &= F_{T_z|H_s}^{-1}\left(\Phi\left(u_2\right)|h(\boldsymbol{u})\right) = \exp\left\{\mu\left(h\left(\boldsymbol{u}\right)\right) + \sigma\left(h\left(\boldsymbol{u}\right)\right)u_2\right\}, \\
v_3(\boldsymbol{u}) &= F_{V_3|T_z,H_s}^{-1}\left(\Phi\left(u_3\right)|h(\boldsymbol{u}), t(\boldsymbol{u})\right).
\end{aligned}$$

Using (28) we find that when $V_3 = \tilde{R}$ we have

$$v_3\left(\boldsymbol{u}\right) = \tilde{r}\left(\boldsymbol{u}\right) = \sqrt{-2m_0\left(h\left(\boldsymbol{u}\right), t\left(\boldsymbol{u}\right)\right)\ln\left(-\frac{2\pi}{\tilde{T}}\sqrt{\frac{m_0\left(h\left(\boldsymbol{u}\right), t\left(\boldsymbol{u}\right)\right)}{m_2\left(h\left(\boldsymbol{u}\right), t\left(\boldsymbol{u}\right)\right)}}\ln\Phi\left(u_3\right)\right)},$$

and in the case $V_3 = Y$ we find from (9) that $F_{Y|\boldsymbol{S}}^{-1}\left(\Phi\left(u_3\right)|\boldsymbol{s}\right) = F_{\tilde{R}|\boldsymbol{S}}^{-1}\left(e^{\Phi(u_3)-1}|\boldsymbol{s}\right)$ which yields

$$v_3\left(\boldsymbol{u}\right) = y\left(\boldsymbol{u}\right) = \sqrt{-2m_0\left(h\left(\boldsymbol{u}\right), t\left(\boldsymbol{u}\right)\right)\ln\left(\frac{2\pi}{\tilde{T}}\sqrt{\frac{m_0\left(h\left(\boldsymbol{u}\right), t\left(\boldsymbol{u}\right)\right)}{m_2\left(h\left(\boldsymbol{u}\right), t\left(\boldsymbol{u}\right)\right)}}\left(1-\Phi\left(u_3\right)\right)\right)}.$$

We note that each evaluation of the function $v_3(\boldsymbol{u})$ requires one short-term response analysis since the response spectrum $S_{R|\boldsymbol{S}}(\omega|\boldsymbol{s})$ must be calculated for the environmental variables $\boldsymbol{s} = [h(\boldsymbol{u}), t(\boldsymbol{u})]$ in order to calculate the required moments $m_0(h(\boldsymbol{u}), t(\boldsymbol{u}))$ and $m_2(h(\boldsymbol{u}), t(\boldsymbol{u}))$. Having established the expression for $v_3(\boldsymbol{u})$ the transformed limit state function $g_r(\boldsymbol{u})$ in (14) is given by

$$g_r(\boldsymbol{u}) = r - v_3(\boldsymbol{u}).$$

6. Numerical results

Algorithm 1 was implemented in MATLAB [22] for calculation of the IFORM approximations to the M-year extreme response of the SDOF example described in Section 5. The IFORM solutions obtained when the exact formulation (2) and the approximate formulation (3) were used are denoted by r_M^{I} and $\bar{r}_M^{\mathrm{I}}$ respectively.

6.1. One-parameter environmental distribution

For illustration purposes we first consider a simplified environmental model obtained by regarding the zero-crossing period T_z as deterministic, given by the conditional median $T_z|H_s = \exp\{\mu(H_s)\}$. This means that H_s is the only environmental variable, and the solution of the IFORM problem (19) can be illustrated in two dimensions. In this case the IFORM problem (19) is that of finding the maximal value of $v_{n+1}(\boldsymbol{u})$ when $\boldsymbol{u}$ is constrained to the circle of radius β. When the exact formulation is used we have that $v_{n+1}(\boldsymbol{u}) = y(\boldsymbol{u})$. For the 100-year response r_{100}^{I} the value of β corresponds to an exceedance probability of $1/(2920 \cdot 100)$ and, as described in Section 4.1, β can be found from (18) as

$$\beta = -\Phi^{-1}\left(-\ln\left[1 - \frac{1}{292000}\right]\right) = 4.498.$$

Figure 5 shows how r_{100}^{I} is obtained for the case $\omega_n = 2.0$ rad/s by using Algorithm 1. The circle of radius β is shown along with the level curves of the function $y(\boldsymbol{u})$, with a colouring corresponding to the value of $y(\boldsymbol{u})$. We observe that after six iterations we have convergence to the optimal point $\boldsymbol{u}^*$

where the level curve of $y(\boldsymbol{u})$ through the point is tangent to the circle. In this case the standard iteration (21) did converge, and the backtracking part of Algorithm 1 remained idle. At $\boldsymbol{u}^* = [4.17, 1.67]$ the function $y(\boldsymbol{u})$ attains its maximal value on the circle, 38.13 m, and the design point is obtained as $\boldsymbol{v}^* = T^{-1}(\boldsymbol{u}^*) = [h^*, y^*] = [8.01 \text{ m}, 38.13 \text{ m}]$. Thus $r^{\mathrm{I}}_{100} = 38.13$ m when the simplified environmental model is used.

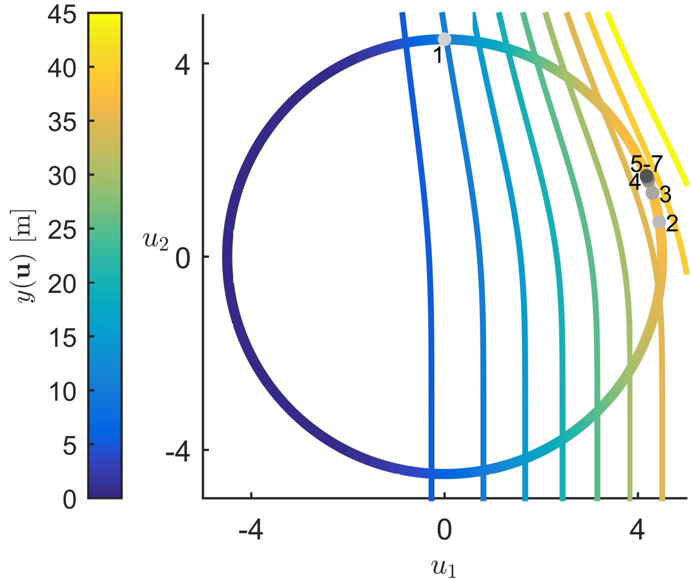

Figure 5: The iteration points obtained when solving the maximization problem (19) for finding the 100-year response r^{I}_{100} in the case that the simplified environmental model is used and $\omega_n = 2.0$ rad/s. The circle of radius β is shown along with the level curves of the function $y(\boldsymbol{u})$, with a colouring corresponding to the value of $y(\boldsymbol{u})$.

6.2. The backtracking approach

In order to demonstrate the need for the backtracking approach in Algorithm 1 for stabilizing the iteration (21), the 100-year response r^{I}_{100} was calculated for the case $\omega_n = 2.0$ rad/s. In Figure 6 it is shown how the maximization problem (19) is solved in an iterative manner. When both H_s and T_z are considered as random variables in the environmental model, we seek the maximal value of $v_{n+1}(\boldsymbol{u})$ on the sphere of radius β. The left part of Figure 6 shows the iteration points obtained when the standard iteration (21) was used, without applying the backtracking approach. In this case the iteration clearly diverges, failing to converge towards the optimal point. The result of employing the backtracking approach is shown to the right in Figure 6. We observe that the backtracking prevents the diverging behaviour and the iteration converges after ten iterations to the optimal point $\boldsymbol{u}^* = [4.09, -0.96, 1.60]$, which yields the design point $\boldsymbol{v}^* = T^{-1}(\boldsymbol{u}^*) = [h^*, t^*, v_3^*] = [7.84 \text{ m}, 2.62 \text{ s}, 40.54 \text{ m}]$ and thus $r_{100}^{\mathrm{I}} = 40.54$ m.

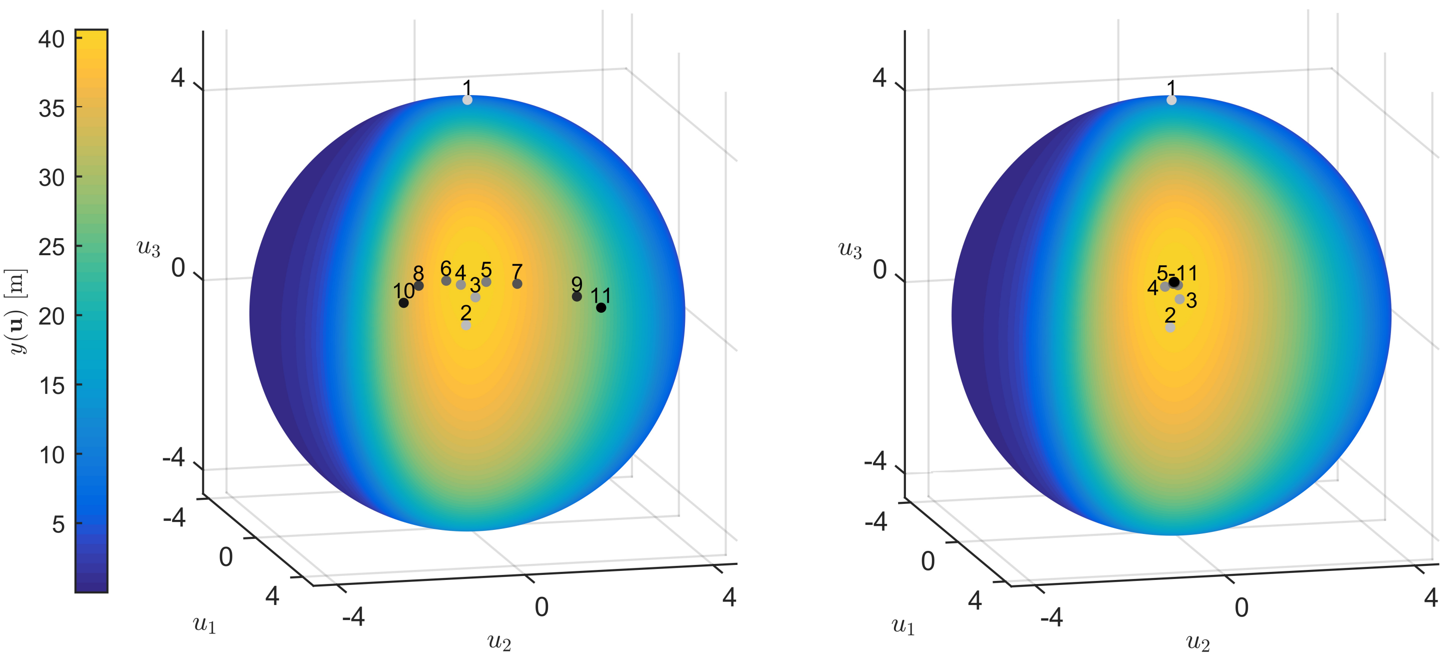

Figure 6: The iteration points obtained when solving the maximization problem (19) for finding the 100-year response r_{100}^{I} in the case $\omega_n = 2.0$ rad/s. The iteration (21) is used with (right) and without (left) the backtracking approach.

6.3. The long-term extreme response approximations

In order to investigate the accuracy of the IFORM approximations r_M^{I} and $\bar{r}_M^{\mathrm{I}}$ for the extreme response, the formulations (2) and (3) were calculated in an exact manner using numerical integration and the exact values r_M and $\bar{r}_M$

were obtained. Thus r_M is the exact M-year extreme response, $\bar{r}_M$ is the extreme response given by the approximate formulation, and r_M^{I} and $\bar{r}_M^{\mathrm{I}}$ are the respective IFORM approximations. We would also like to investigate how accurate the approximate formulation (3) is with respect to extreme responses.

In Table 1, Table 2 and Table 3 the M-year extreme response r_M and its approximations are calculated for $M = 10$, $M = 100$ and $M = 1000$ respectively, and the relative errors of the approximations are also displayed. The extreme response is calculated for different values of ω_n, thereby varying the characteristics of the SDOF system. Also, for the IFORM approximations the number of required short-term response calculations n_{st} is given, i.e. the number of evaluations of the function $v_{n+1}(\boldsymbol{u})$ in Algorithm 1. For each iteration $n+2$ evaluations are needed to calculate $v_{n+1}(\boldsymbol{u}^k)$ and $\nabla v_{n+1}(\boldsymbol{u}^k)$ using a finite difference approximation, in addition to the evaluations of $v_{n+1}(\boldsymbol{u}^{k+1})$ which is one for each backtracking step.

Comparing the results obtained using full numerical integration we see that the approximate formulation (3) does indeed underestimate the extreme response values, demonstrating what was shown in Section 2.3. However, the error of the approximation is in most cases within a few percent, and it decreases with increasing return period, i.e. decreasing exceedance probability.

For the IFORM approximations we notice that the difference between using the exact and the approximate formulation is in fact very small, and both IFORM methods give reasonably good estimates for the M-year response r_M. In most of the cases considered here, using IFORM actually improves the estimate compared to full integration of the approximate formulation. However, whether this is the case will be structure dependent. Regarding the number of short-term structural response analyses n_{st}, this appears to be around 50, although some cases display faster or slower convergence resulting in smaller or larger values of n_{st}. This number of analyses is expected to be the same if a more complex structure is considered, making a full long-term response analysis feasible also when short-term response calculations are time demanding.

Finally, a plot showing the design points obtained in the calculation of the

Table 1: The 10-year extreme response r_M, $M = 10$, and its approximations $\bar{r}_M$, r_M^{I} and $\bar{r}_M^{\mathrm{I}}$, along with the relative errors of the approximations. For the IFORM approximations the number of required short-term response calculations n_{st} is also given.

	Full integration			IFORM approximations					
	Ex. for.	Approx. for.		Exact formulation			Approximate formulation		
ω_n [rad/s]	r_M [m]	$\bar{r}_M$ [m]	$\frac{\bar{r}_M - r_M}{r_M}$	r_M^{I} [m]	$\frac{r_M^{\mathrm{I}} - r_M}{r_M}$	n_{st}	$\bar{r}_M^{\mathrm{I}}$ [m]	$\frac{\bar{r}_M^{\mathrm{I}} - r_M}{r_M}$	n_{st}
0.5	9.78	8.29	−15.2%	9.63	−1.5%	117	9.53	−2.5%	105
1.0	26.97	25.84	−4.2%	27.37	1.5%	74	27.27	1.1%	64
1.5	35.96	34.74	−3.4%	36.04	0.2%	68	35.94	−0.1%	59
2.0	35.46	34.33	−3.2%	35.39	−0.2%	47	35.30	−0.4%	38
2.5	31.69	30.69	−3.2%	31.54	−0.5%	45	31.45	−0.8%	37
4.0	21.18	20.32	−4.1%	20.79	−1.9%	30	20.71	−2.2%	27
6.0	13.79	13.01	−5.7%	13.01	−5.7%	41	12.94	−6.2%	37
∞	8.54	8.28	−3.0%	8.26	−3.2%	25	8.24	−3.5%	21

IFORM approximations r_M^{I} is given in Figure 7 along with the distribution of the environmental parameters. This demonstrates that the IFORM solution by Algorithm 1 also produces a set of environmental variables representing the main contribution to the long-term extreme response, and this set can be quite different for the different cases.

7. Concluding remarks

An exact and an approximate formulation for the long-term extreme response of marine structures have been discussed and compared in this paper. It has been shown that the approximate formulation is non-conservative in the sense that it underestimates the long-term extreme response values. It has also been shown how both formulations can be solved in an approximate manner using FORM, and extreme response values can be obtained by IFORM. Finally, a new solution algorithm for the IFORM problem has been proposed which resolves some convergence issues of a well-established iteration algorithm.

Table 2: The 100-year extreme response r_M, $M = 100$, and its approximations $\bar{r}_M$, r^{I}_M and $\bar{r}^{\mathrm{I}}_M$, along with the relative errors of the approximations. For the IFORM approximations the number of required short-term response calculations n_{st} is also given.

	Full integration			IFORM approximations					
	Ex. for.	Approx. for.		Exact formulation			Approximate formulation		
ω_n [rad/s]	r_M [m]	$\bar{r}_M$ [m]	$\frac{\bar{r}_M - r_M}{r_M}$	r^{I}_M [m]	$\frac{r^{\mathrm{I}}_M - r_M}{r_M}$	n_{st}	$\bar{r}^{\mathrm{I}}_M$ [m]	$\frac{\bar{r}^{\mathrm{I}}_M - r_M}{r_M}$	n_{st}
0.5	11.93	11.06	−7.3%	12.45	4.3%	124	12.38	3.7 %	105
1.0	31.06	30.43	−2.0%	31.88	2.6%	85	31.83	2.5 %	75
1.5	41.00	40.31	−1.7%	41.53	1.3%	63	41.48	1.2 %	54
2.0	40.22	39.60	−1.5%	40.59	0.9%	47	40.54	0.8 %	38
2.5	35.86	35.31	−1.5%	36.11	0.7%	46	36.07	0.6 %	37
4.0	23.98	23.49	−2.0%	24.00	0.1%	47	23.96	−0.1 %	38
6.0	15.70	15.17	−3.4%	15.39	−2.0%	53	15.34	−2.3 %	48
∞	9.67	9.52	−1.5%	9.49	−1.8%	29	9.48	−1.9 %	21

Table 3: The 1000-year extreme response r_M, $M = 1000$, and its approximations $\bar{r}_M$, r^{I}_M and $\bar{r}^{\mathrm{I}}_M$, along with the relative errors of the approximations. For the IFORM approximations the number of required short-term response calculations n_{st} is also given.

	Full integration			IFORM approximations					
	Ex. for.	Approx. for.		Exact formulation			Approximate formulation		
ω_n [rad/s]	r_M [m]	$\bar{r}_M$ [m]	$\frac{\bar{r}_M - r_M}{r_M}$	r^{I}_M [m]	$\frac{r^{\mathrm{I}}_M - r_M}{r_M}$	n_{st}	$\bar{r}^{\mathrm{I}}_M$ [m]	$\frac{\bar{r}^{\mathrm{I}}_M - r_M}{r_M}$	n_{st}
0.5	14.13	13.64	−3.5%	15.05	6.5%	135	15.01	6.2%	90
1.0	35.21	34.86	−1.0%	36.29	3.1%	85	36.27	3.0%	75
1.5	46.09	45.73	−0.8%	46.92	1.8%	53	46.90	1.7%	43
2.0	45.03	44.71	−0.7%	45.68	1.4%	47	45.66	1.4%	42
2.5	40.07	39.78	−0.7%	40.57	1.3%	42	40.55	1.2%	42
4.0	26.79	26.53	−1.0%	27.09	1.1%	48	27.07	1.0%	48
6.0	17.65	17.31	−1.9%	17.70	0.3%	75	17.67	0.1%	65
∞	10.81	10.73	−0.7%	10.70	−1.0%	26	10.70	−1.0%	25

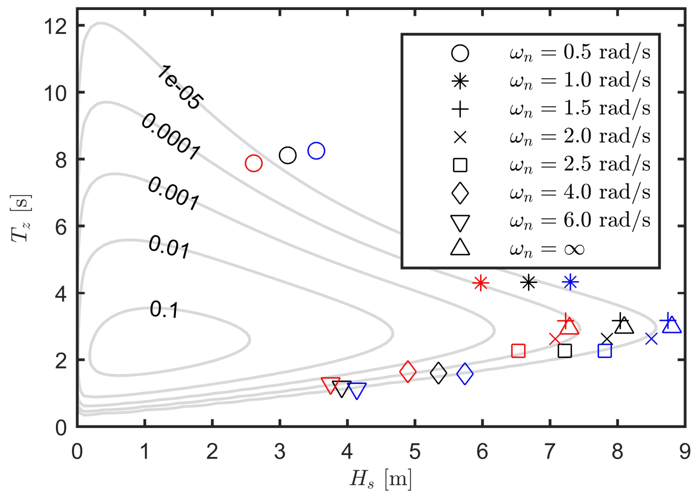

Figure 7: The design points corresponding to the M-year response for $M = 10$ (red), $M = 100$ (black) and $M = 1000$ (blue), along with the PDF of the environmental parameters.

Numerical results have also been presented, demonstrating the proposed solution algorithm and comparing it with the standard iteration algorithm. The different approximations for the long-term extreme response have been compared for an SDOF example in order to assess the accuracy of the approximations. It is found that both IFORM approximations give reasonably good estimates for the long-term extreme response. The number of required short-term response analyses for the IFORM method is found to be within acceptable limits, making a full long-term extreme response analysis feasible also for more complex structures.

Acknowledgements

The authors are grateful for grants which are provided by Multiconsult ASA and the Research Council of Norway.

References

[1] Naess A, Moan T. Stochastic dynamics of marine structures. Cambridge: Cambridge University Press; 2012. ISBN 9781139021364. URL:

http://ebooks.cambridge.org/ebook.jsf?bid=CBO9781139021364. doi:10.1017/CBO9781139021364.

[2] Sagrilo L, Naess A, Doria A. On the long-term response of marine structures. Appl Ocean Res 2011;33(3):208–14. URL: http://www.sciencedirect.com/science/article/pii/S0141118711000204. doi:10.1016/j.apor.2011.02.005.

[3] Winterstein SR, Ude TC, Cornell CA, Bjerager P, Haver S. Environmental parameters for extreme response: inverse FORM with omission factors. In: Proc. 6th Int. Conf. Struct. Saf. Reliab. Innsbruck, Austria; 1993,URL: http://www.rms-group.org/RMS_Papers/pdf/Todd/innsbruck.pdf.

[4] Haver S, Kleiven G. Environmental contour lines for design purposes: why and when? ASME Conf Proc 2004;2004(37432):337–45. URL: http://proceedings.asmedigitalcollection.asme.org/proceeding.aspx?articleid=1628932. doi:10.1115/OMAE2004-51157.

[5] Haver S, Winterstein S. Environmental contour lines: a method for estimating long term extremes by a short term analysis. Trans Soc Nav Archit Mar Eng 2010;116(October):116–27. URL: http://www.sname.org/HigherLogic/System/DownloadDocumentFile.ashx?DocumentFileKey=ccb5aac7-6b77-420b-b233-836fc6e13597.

[6] Vázquez-Hernández A, Ellwanger G, Sagrilo L. Long-term response analysis of FPSO mooring systems. Appl Ocean Res 2011;33(4):375–83. URL: http://www.sciencedirect.com/science/article/pii/S0141118711000472. doi:10.1016/j.apor.2011.05.003.

[7] Zhang Y, Beer M, Quek ST. Long-term performance assessment and design of offshore structures. Comput Struct 2015;154:101–15. URL: http://www.sciencedirect.com/science/article/pii/S004579491500067X. doi:10.1016/j.compstruc.2015.02.029.

[8] Naess A, Gaidai O, Teigen P. Extreme response prediction for nonlinear floating offshore structures by Monte Carlo simulation. Appl Ocean Res 2007;29(4):221–30. URL: http://www.sciencedirect.com/science/article/pii/S0141118708000035. doi:10.1016/j.apor.2007.12.001.

[9] Naess A, Gaidai O. Monte Carlo methods for estimating the extreme response of dynamical systems. J Eng Mech 2008;134(8):628–36. URL: http://ascelibrary.org/doi/full/10.1061/(ASCE)0733-9399(2008)134%3A8(628). doi:10.1061/(ASCE)0733-9399(2008)134:8(628).

[10] Giske FIG, Leira BJ, Øiseth O. Efficient computation of cross-spectral densities in the stochastic modelling of waves and wave loads. Appl Ocean Res 2016;doi:10.1016/j.apor.2016.11.007.

[11] Der Kiureghian A, Zhang Y, Li CC. Inverse reliability problem. J Eng Mech 1994;120(5):1154–9. URL: http://ascelibrary.org/doi/10.1061/%28ASCE%290733-9399%281994%29120%3A5%281154%29. doi:10.1061/(ASCE)0733-9399(1994)120:5(1154).

[12] Li H, Foschi RO. An inverse reliability method and its application. Struct Saf 1998;20(3):257–70. URL: http://www.sciencedirect.com/science/article/pii/S0167473098000101. doi:10.1016/S0167-4730(98)00010-1.

[13] Du X, Sudjianto A, Chen W. An integrated framework for optimization under uncertainty using inverse reliability strategy. J Mech Des 2004;126(4):562–70. URL: http://mechanicaldesign.asmedigitalcollection.asme.org/article.aspx?articleid=1448186. doi:10.1115/1.1759358.

[14] Naess A. Technical note: On the long-term statistics of extremes. Appl Ocean Res 1984;6(4):227–8. URL: http://www.sciencedirect.com/science/article/pii/0141118784900610. doi:10.1016/0141-1187(84)90061-0.

[15] Krogstad HE. Height and period distributions of extreme waves. Appl Ocean Res 1985;7(3):158–65. doi:10.1016/0141-1187(85)90008-2.

[16] Melchers RE. Structural reliability analysis and prediction. 2nd ed.; John Wiley & Sons; 1999. ISBN 9780471987710.

[17] Nocedal J, Wright SJ. Numerical optimization. Springer series in operations research and financial engineering; 2nd ed.; Springer New York; 2006. ISBN 9780387400655. URL: http://link.springer.com/10.1007/978-0-387-40065-5. doi:10.1007/978-0-387-40065-5.

[18] Armijo L. Minimization of functions having Lipschitz continuous first partial derivatives. Pacific J Math 1966;16(1):1–3. URL: http://projecteuclid.org/euclid.pjm/1102995080$\delimiter"026E30F$nhttps://projecteuclid.org/euclid.pjm/1102995080. doi:10.2140/pjm.1966.16.1.

[19] Stansberg CT, Contento G, Hong SW, Irani M, Ishida S, Mercier R, et al. The specialist committee on waves final report and recommendations to the 23rd ITTC. In: Proceedings of the 23rd ITTC. 2002, p. 505–736. URL: http://ittc.info/media/1469/waves.pdf.

[20] DNV . DNV-RP-C205 Environmental conditions and environmental loads. Tech. Rep. October; DNV; Høvik, Norway; 2010. URL: https://rules.dnvgl.com/docs/pdf/DNV/codes/docs/2010-10/RP-C205.pdf.

[21] Bitner-Gregersen EM, Haver S. Joint environmental model for reliability calculations. In: Proc. First Int. Offshore Polar Eng. Conf. Edinburgh, United Kingdom: International Society of Offshore and Polar Engineers; 1991, p. 246–53. URL: https://www.onepetro.org/conference-paper/ISOPE-I-91-031.

[22] The MathWorks Inc. . MATLAB Release 2015a. 2015.